membranes

MDPI

Article

Advanced Membrane Processes for the Removal of Anthelmintics, Neonicotinoids and Their Mixtures: Retention Mechanisms and Effects on Ecotoxicity

Bruna Babić Visković [1,*], Petra Mustapić [1], Veronika Stepan [1], Danijela Ašperger [1] and Davor Dolar [2]

[1] Department of Analytical Chemistry, University of Zagreb Faculty of Chemical Engineering and Technology, Marulićev trg 19, 10000 Zagreb, Croatia; pmustapic@fkit.unizg.hr (P.M.); vstepan@fkit.unizg.hr (V.S.); diva@fkit.unizg.hr (D.A.)
[2] Department of Physical Chemistry, University of Zagreb Faculty of Chemical Engineering and Technology, Marulićev trg 19, 10000 Zagreb, Croatia; dolar@fkit.unizg.hr
* Correspondence: bbabic@fkit.unizg.hr; Tel.: +385-1-4597-207

Abstract

Veterinary anthelmintics and neonicotinoid insecticides in aquatic environments pose challenges for conventional wastewater treatment. Six commercial ultrafiltration (UF), nanofiltration (NF), and reverse osmosis (RO) membranes were evaluated for the rejection of three veterinary anthelmintics (albendazole, febantel, and mebendazole) and three neonicotinoid insecticides (acetamiprid, clothianidin, and thiacloprid). The compounds were tested individually and as a six-component mixture in demineralized and model water. After 3 h, rejection of the individual compounds was at least 92.9% with the tight NF membrane ESNA1-LF-LD and 94.1% with the RO membrane ESPA4. Neonicotinoid rejection by the UF membrane did not exceed 9.2%. In the six-component mixture, ESNA1-LF-LD rejected 87.9–94.9% of neonicotinoids and 90.1% to >99.9% of anthelmintics. The RO membranes (XLE and ESPA4) rejected 89.8–94.8% of neonicotinoids and 92.5% to >99.9% of anthelmintics. Fourier transform infrared (FTIR) spectroscopy indicated possible interactions between anthelmintics and the membranes. At the highest sample volume fraction tested, the untreated mixture caused 63.6% inhibition of *Vibrio fischeri* bioluminescence in demineralized water and 86.8% in model water. No inhibition was detected in the XLE or ESPA4 permeates. Rejection depended on membrane selectivity, compound properties, and water matrix. Combining chemical measurements with ecotoxicity assays provided a broader assessment of membrane treatment performance.

Keywords: anthelmintics; neonicotinoids; membrane processes; removal mechanisms; ecotoxicity

Check for updates

Academic Editor: Xue Jin

Received: 13 October 2026
Revised: 16 November 2026
Accepted: 19 November 2026
Published: 20 November 2026

Copyright: © 2026 by the authors. Licensee MDPI, Basel, Switzerland. This article is an open access article distributed under the terms and conditions of the Creative Commons Attribution (CC BY) license.

1. Introduction

Water resources are under increasing pressure from the rising consumption of chemical substances, among which xenobiotics, compounds foreign to biological systems, occupy a special place, as their presence is now recorded in almost all environmental matrices [1–3]. Their growing occurrence in aquatic systems is a serious environmental concern, since many of these compounds exhibit high persistence, limited biodegradability and a pronounced tendency to bioaccumulate, enabling them to enter food chains and exert chronic toxic effects on organisms and ecosystems [1,4].

Over the past two decades, the use of veterinary and human pharmaceuticals, pesticides and numerous other synthetic substances has expanded markedly, resulting in their

pseudo-persistent presence in surface water, groundwater, soil and sediments [4,5]. Among pharmaceuticals, anthelmintics are of particular concern, as they have become some of the most frequently detected antiparasitic compounds in the environment due to their intensive use in livestock, aquaculture and human medicine [6–8]. Anthelmintics are widely used veterinary and human pharmaceuticals for the control of parasitic infections, with benzimidazole derivatives such as albendazole, mebendazole, and febantel among the most commonly applied compounds [8–15]. Due to their extensive application in livestock production, substantial fractions of administered doses are excreted unmetabolised or as biologically active metabolites and subsequently released into the environment via manure, agricultural runoff and wastewater treatment plants [16,17]. It is estimated that up to 50% of applied anthelmintics may ultimately reach aquatic systems [17]. Numerous studies have confirmed the widespread occurrence of these compounds and their metabolites in wastewater, soils, sediments, and natural waters [18–22]. Albendazole and its metabolites (albendazole sulfoxide, sulfone, and 2-aminosulfone) are among the most frequently detected compounds, while mebendazole exhibits pronounced lipophilicity and persistence, and febantel enters the environment primarily through its active metabolites, fenbendazole and oxfendazole [12,23]. Their continuous input into the environment leads to pseudo-persistent contamination and contributes to the development of antiparasitic resistance, posing a growing challenge for both environmental and public health [24–27]. In addition, recent trends in the repurposing of anthelmintics, particularly albendazole and mebendazole, in oncology have increased their overall consumption, thereby amplifying their environmental footprint [28–33].

Pesticides constitute another large group of xenobiotics with significant environmental impacts [34–39]. Within this group, neonicotinoid insecticides such as acetamiprid, clothianidin, and thiacloprid have attracted particular attention due to their high insecticidal efficacy, systemic activity and wide agricultural application [40–46]. Although originally developed as more environmentally friendly alternatives to older classes of pesticides, neonicotinoids have shown toxicity to non-target organisms due to their high solubility, chemical stability, mobility and persistence in aquatic environments, and they have been detected in surface waters, groundwater, and drinking water worldwide [35,47,48]. Their environmental stability and resistance to biodegradation contribute to their long-term presence in water bodies and potential adverse effects on non-target organisms [40–48].

Conventional wastewater treatment plants (WWTPs), based primarily on primary and secondary treatment processes, are generally inefficient at removing pharmaceuticals, pesticides and other organic micropollutants [1,7]. Their limited removal efficiency largely stems from the physico-chemical properties of these compounds, including molecular size, polarity, ionization behavior, hydrophobicity and high persistence, which reduce their susceptibility to conventional treatment processes [1,7,23]. In particular, biological treatment, the core process in most municipal WWTPs, is often unable to effectively degrade persistent xenobiotics, resulting in their continuous release into receiving aquatic environments [17,49].

The revised European Union Urban Wastewater Treatment Directive recognizes pharmaceuticals and pesticides as priority micropollutants and requires the implementation of advanced treatment technologies, further emphasizing the need for efficient removal processes. Among the available advanced treatment options, membrane separation processes have emerged as particularly promising tools for removing pesticides and pharmaceutical residues from water [50–54]. Pressure-driven membrane processes, including ultrafiltration (UF), nanofiltration (NF), and reverse osmosis (RO), are established technologies in water and wastewater treatment. For organic micropollutants, removal efficiency generally increases in the order UF < NF < RO [54].

Numerous studies have demonstrated the potential of NF and RO for removing pesticides and pharmaceutical residues from different water matrices [18,55–60]. In these

studies, NF and RO have consistently achieved removal efficiencies exceeding 90%, with RO generally outperforming NF due to its smaller effective pore size and higher selectivity [55–60]. Membrane retention depends not only on membrane characteristics but also on the physico-chemical properties of target compounds, including molecular size, molecular weight, ionization behavior, hydrophobicity, and charge, as well as on the composition of the treated water matrix [59,61,62]. High removal efficiencies have been reported for both neonicotinoid insecticides and benzimidazole anthelmintics. For example, Dolar et al. demonstrated efficient rejection of albendazole, febantel, and their photodegradation products using both NF and RO membranes, with RO providing the highest rejection rates [18,54]. A separate study by Dolar et al. [63] showed that the composition of the water matrix affected the rejection of veterinary pharmaceuticals, including febantel. Babić et al. [64] reported mebendazole rejection above 97.7% with NF90 and XLE membranes and evaluated bioluminescence inhibition before and after photolysis. Racar et al. [53] showed that NF or RO improved micropollutant removal when applied after a membrane bioreactor.

To help meet the quaternary treatment requirements of the revised European Union Urban Wastewater Treatment Directive, membrane filtration may be added to existing urban wastewater treatment schemes, for example as a polishing step after biological treatment. Studies have shown that combining biological treatment, membrane separation, and advanced oxidation processes (AOPs) can improve the removal of both parent compounds and their transformation products and reduce the resulting ecotoxicity [18,20]. Such integrated treatment strategies represent a promising and sustainable approach for the effective control of pesticide and pharmaceutical contamination in aquatic environments.

Xenobiotics can occur together in water bodies, making it important to determine whether the removal measured for individual compounds is representative of their behaviour in mixtures. Single-compound experiments provide a baseline for each solute, while mixture experiments reveal how rejection changes when other contaminants are present. Previous work has shown that membrane rejection can differ between single-solute and mixed-solute feeds [65]. The novelty of the present study lies in directly comparing the rejection of the same six xenobiotics tested individually and together in a mixture of veterinary anthelmintics and neonicotinoid insecticides, two classes with contrasting physico-chemical properties. Testing these solutions across six commercial UF, NF, and RO membranes in both demineralized and model water allowed us to determine whether differences between single-compound and mixture experiments were consistent across membranes and water matrices. The model water provided a controlled way to examine the influence of dissolved constituents relevant to natural waters.

Changes in acute ecotoxicity following membrane filtration were evaluated by measuring *Vibrio fischeri* bioluminescence inhibition in the initial solutions and their corresponding permeates. This comparison showed how the inhibitory effects of the individual compounds and their mixture changed after treatment in each water matrix. By capturing the bacterial response to each sample as a whole, the bioassay complemented the chemical analysis and provided a more complete assessment of membrane treatment performance.

2. Materials and Methods

2.1. Chemicals

All chemicals used in this study are listed in Table S1. Analytical grade reagents were used unless otherwise stated. Ultra-pure water obtained from a Milli-Q purification system (Millipore, Burlington, MA, USA) was used to prepare all solutions.

Six xenobiotics were investigated, including three anthelmintics (albendazole, febantel, and mebendazole) and three pesticides (acetamiprid, clothianidin, and thiacloprid). The anthelmintics febantel and albendazole were supplied by Veterina d.d. (Kalinovica, Croatia),

while mebendazole was obtained from Acros Organics (Geel, Belgium). The pesticides were purchased from Sigma-Aldrich (St. Louis, MO, USA). All compounds had purity ≥ 98%.

The physico-chemical properties of the investigated xenobiotics are summarized in Tables 1 and 2.

Table 1. Physico-chemical and general properties of anthelmintics.

Xenobiotic	Albendazole	Febantel	Mebendazole
CAS number	54965-21-8	58306-30-2	31431-39-7
Formula	$C_{12}H_{15}N_3O_2S$	$C_{20}H_{22}N_4O_6S$	$C_{16}H_{13}N_3O_3$
M_w (g/mol)	265.33	446.48	295.30
Molecular structures	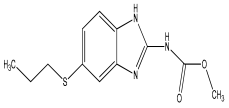	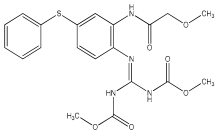	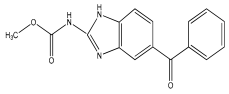
Width (nm) [a]	X = 0.482	X = 1.058	X = 0.511
Height (nm) [a]	Y = 0.279	Y = 0.651	Y = 0.418
Length (nm) [a]	Z = 1.632	Z = 1.292	Z = 1.572
Dipole moment [a]	4.3 D	6.3 D	6.3 D
3D representation and orientation of the dipole moment [b]		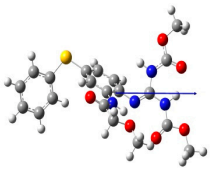	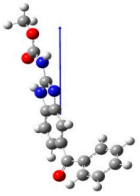
log $K_{O/W}$	3.07[18]	1.53[18]	2.83 [c]
pK_a	9.93; 3.37 [d]	7.60 [e]	8.44; 3.93 [f]
t_t (°C) [c]	192.24	258.19	223.41
t_v (°C) [c]	472.79	597.61	523.14
S (mg/L)	10.00 [g]	76.92 [c]	71.30 [c]

[a]—dipole moment calculated by Gauss's method; [b]—HyperChem professional program; [c]—EPISuite 4.11; [d]—[23] [e]—https://www.chemicalbook.com/ChemicalProductProperty_EN_CB2502427.htm (accessed on 19 June 2025); [f]—https://go.drugbank.com/drugs/DB00643 (accessed on 19 June 2025); [g]—[66].

Table 2. Physico-chemical and general properties of pesticides.

Xenobiotic	Acetamiprid	Clothianidin	Thiacloprid
CAS number	135410-20-7	210880-92-5	111988-49-9
Formula	$C_{10}H_{11}ClN_4$	C6H8ClN$_5$O$_2$S	$C_{10}H_9ClN_4S$
M_w (g/mol)	222.67	249.68	252.72
Molecular structures	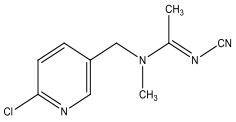	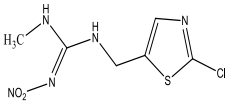	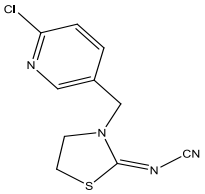
Width (nm) [a]	X = 0.627	X = 0.625	X = 0.630
Height (nm) [a]	Y = 0.370	Y = 0.464	Y = 0.469
Length (nm) [a]	Z = 0.942	Z = 0.810	Z = 0.751
Dipole moment [a]	4.8 D	3.9 D	6.4 D
3D representation and orientation of the dipole moment [b]	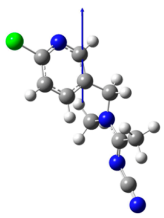	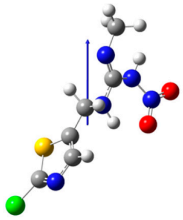	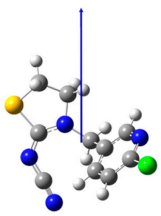
log $K_{O/W}$ [e]	0.80	0.91	1.26
pK_a	-	11.10 [d]	-

Table 2. *Cont.*

Xenobiotic	Acetamiprid	Clothianidin	Thiacloprid
t_t (°C) [c]	106.78	146.49	150.44
t_v (°C) [c]	339.97	363.86	383.00
S (mg/L) [e]	2950.00	340.00	184.00

[a]—dipole moment calculated by Gauss's method; [b]—HyperChem professional program; [c]—EPISuite 4.11; [d]—[62]; [e]—[67].

Stock standard solutions were prepared by dissolving accurately weighed amounts of xenobiotics in appropriate solvents. Pesticides stock solutions (100 mg/L) were dissolved in Milli-Q water using an ultrasonic bath, while anthelmintics (400 mg/L) and the mixture of xenobiotics were dissolved in methanol. Stock solutions were stored in the dark at 4 °C.

Working solutions with a concentration of 10 mg/L were prepared daily by diluting the stock solutions with demineralized water or model solution. The composition of the model solution is given in Table S2.

2.2. Membranes

Removal of xenobiotics was investigated using commercial UF, NF, and RO membranes obtained from different manufacturers. The tested membranes included GH (UF), NF, DK and ESNA1-LF-LD (NF), and XLE and ESPA4 (RO). Their main characteristics are presented in Tables 3 and S3.

Table 3. Nominal properties of tested commercial membranes according to manufacturer.

Characteristic	GH	NF	DK	ESNA1-LF-LD	XLE	ESPA4
MWCO, Da	2500	200–400	150–300	-	100	-
Working pressure, bar	11.0	-	7.6	5.2	8.6	7
Salt retention factor	n.d.	n.d.	0.98 $MgSO_4$	0.97 $CaCl_2$	0.99 NaCl	0.99 NaCl
Permeate flow, L/(m^2·h)	34.3	56.1	39.8	40.3	53.9	50.9
Maximum working pressure, bar	27.6	41.0	41.0	41.4	41.0	41.4
Maximum working temp., °C	50	45	45	45	45	45
Permissible pH-values	2–10	2–11	2–11	2–10	2–11	2–10
Permissible free chlorine concentration, mg/L	-	<0.1	<0.1	<0.1	<0.1	<0.1

Membrane experiments were conducted using a laboratory-scale membrane unit consisting of six parallel connected RO/NF cells and details have been previously published in Dolar et al. (2011) [63]. Each cell contained a flat-sheet membrane with an effective surface area of 11 cm^2. For each experiment, the initial feed volume was 5 L. The feed solution was continuously pumped from the reservoir at a flow rate of 750 mL/min using a high-pressure pump and flowed tangentially across the membrane surface, allowing continuous permeate to be collected. Experiments were performed in batch circulation mode, meaning that permeate and retentate were recirculated back to the feed tank, except when samples (up to 2 mL) were taken for chromatographic analysis. Samples were taken every hour for three hours of treatment.

2.3. Ecotoxicity Test

Ecotoxicity was assessed using the bioluminescent bacterium *Vibrio fischeri* with the LCK484 test kit (Hach Lange GmbH, Düsseldorf, Germany). The test was performed using a LUMIStox 300 instrument in combination with a LUMIStherm incubation block (Dr. Lange

GmbH, Berlin, Germany). The method complies with the technical requirements of DIN 38412 L34 and L341 standards as well as the international standard ISO 11348-1:2007 [68–70].

The lyophilized culture of *Vibrio fischeri* was stored at −18 to −20 °C, while fresh bacterial cultures used for toxicity testing were maintained on a microbial growth medium at 18 °C for 48 h. Sample toxicity was determined using a geometric dilution series in the 2% NaCl solution. The detailed methodology has been previously reported in our earlier study [64].

The ecotoxicity of xenobiotics was evaluated at an initial concentration of 10 mg/L, and toxicity was additionally analyzed after membrane treatment.

2.4. Chemical Analysis

Samples were analysed using an Agilent 1260 Infinity II HPLC system (Agilent Technologies, Santa Clara, CA, USA) equipped with a degasser, quaternary pump (G7111B), autosampler (G7129A), thermostated column compartment (G7116A), and diode array detector (DAD). Data acquisition and processing were performed using OpenLab CDS software version 2.8.

Chromatographic separation was carried out on an Eclipse XDB-C8 column (2.1 mm × 150 mm, 5 µm; Agilent Technologies, Santa Clara, CA, USA). The mobile phase consisted of Milli-Q water (A) and acetonitrile (B). The injection volume was 30 µL and the flow rate was 0.5 mL/min, with a maximum system pressure of 600 bar. Both the autosampler and the column compartment were maintained at 25 °C.

The total analysis time was 15 min, and the gradient elution program was as follows: the initial composition was 10% B, which increased linearly to 40% B within 7 min and to 50% B at 9 min. The acetonitrile content was further increased to 90% B at 11 min, followed by a return to the initial composition (10% B) at 13 min, which was maintained until the end of the analysis at 15 min.

Before and after sample analysis, the column was flushed with 65% acetonitrile at a flow rate of 0.5 mL/min.

Chromatograms were recorded at five wavelengths (210, 241, 245, 254, and 265 nm). Peak areas obtained from standard solutions and analyzed samples were used to determine xenobiotic concentrations and calculate removal efficiencies during the investigated processes.

The analytical method was validated by determining key performance parameters including linearity, sensitivity, repeatability, intermediate precision, recovery, and the limits of detection (LOD) and quantification (LOQ).

2.5. Devices for Membrane Characterization

2.5.1. Fourier Transformation Infrared Spectrometer

Possible interactions between the membranes and xenobiotics were investigated using Fourier transform infrared spectroscopy (FTIR). Measurements were performed using a Vertex 70 FTIR spectrometer (Bruker Corporation, Billerica, MA, USA) equipped with an attenuated total reflection (ATR) accessory with a diamond crystal. Spectra were recorded in the mid-infrared region.

Prior to analysis, membrane samples (≈0.5 × 0.5 cm) were placed on the ATR crystal and a background spectrum (air) was recorded to minimize measurement errors. FTIR spectra were collected in the range of 400–4000 1/cm with a resolution of 4 cm^{-1} and 32 scans.

2.5.2. Electrokinetic Analysis

The zeta potential of the membranes was determined using a SurPASS Electrokinetic Analyzer (Anton Paar, Graz, Austria) with a 0.0001 mol/L KCl electrolyte solution.

Prior to measurement, membrane samples were cut to fit the sample holders (2 × 1 cm) and mounted in the measuring cell with an adjustable gap of 120–130 µm. The system was rinsed with deionized water before to analysis to ensure stable measurement conditions.

Measurements were performed at a pressure of 200 mbar and a volumetric flow rate of 120–130 mL/min. The zeta potential was determined as a function of pH-value in the range of 2–9. The pH-value was adjusted using 0.1 mol/L HCl solution.

2.5.3. Goniometric Analysis

The surface hydrophilicity/hydrophobicity of the selected membranes was evaluated by measuring the water contact angle using a DataPhysics OCA 20 goniometer (DataPhysics Instruments, Filderstadt, Germany). Measurements were performed using the sessile drop method with a droplet volume of 2 µL at a temperature of 20.0 ± 0.1 °C.

The surface free energy of the membranes was calculated from the measured contact angle using the Young-Dupréova equation (Equation (1)):

$$\cos \theta_C = \frac{\gamma_{SL} + \gamma_{LG}}{\gamma_{SG}} \quad (1)$$

where γ_{SG} represents the interfacial energy between the membrane and air, γ_{SL} he interfacial energy between the liquid and the membrane, γ_{LG} the interfacial energy between the liquid and air, and θ_C the equilibrium contact angle.

3. Results and Discussion

3.1. Characterization of UF/NF/RO Membranes

The basic nominal properties of the membranes used by the manufacturer are shown in Tables 3 and S3. However, to facilitate understanding of the removal efficiency and mechanism of xenobiotic removal, the charge and hydrophilicity of the membranes were determined using zeta potential and contact angle measurements, respectively. The results are shown in Figure 1 and in Table 4.

Table 4. Contact angle of the tested membranes.

Membranes	Contact Angle, °
GH	52.7
NF	35.0
DK	52.9
ESNA1-LF-LD	62.8
XLE	65.3
ESPA4	40.1

The charge of the membranes used helps to define the Donnan effect, i.e., the mechanism of electrostatic repulsion or attraction between the membranes and the tested xenobiotics. Based on the obtained results (Figure 1), it can be concluded that all membranes are negatively charged over almost the entire pH-range, except in strongly acidic condition (pH < 3) where they are slightly positively charged. The isoelectric points (IEPs) were estimated by linear interpolation between adjacent measurements bracketing zero zeta potential (Figure 1). The estimated IEPs were 2.8, 3.1, 3.7, 2.5, 3.7, and 3.2 for GH, NF, DK, ESNA1-LF-LD, XLE, and ESPA4, respectively. All six membranes exhibited negative zeta potentials in the pH range of 6–8. In this range, Donnan exclusion may contribute to the rejection of negatively charged solutes, depending on their ionisation state. Electrostatic

interactions become significant when the membrane and the xenobiotics to be removed are oppositely charged [71] (Figure 1).

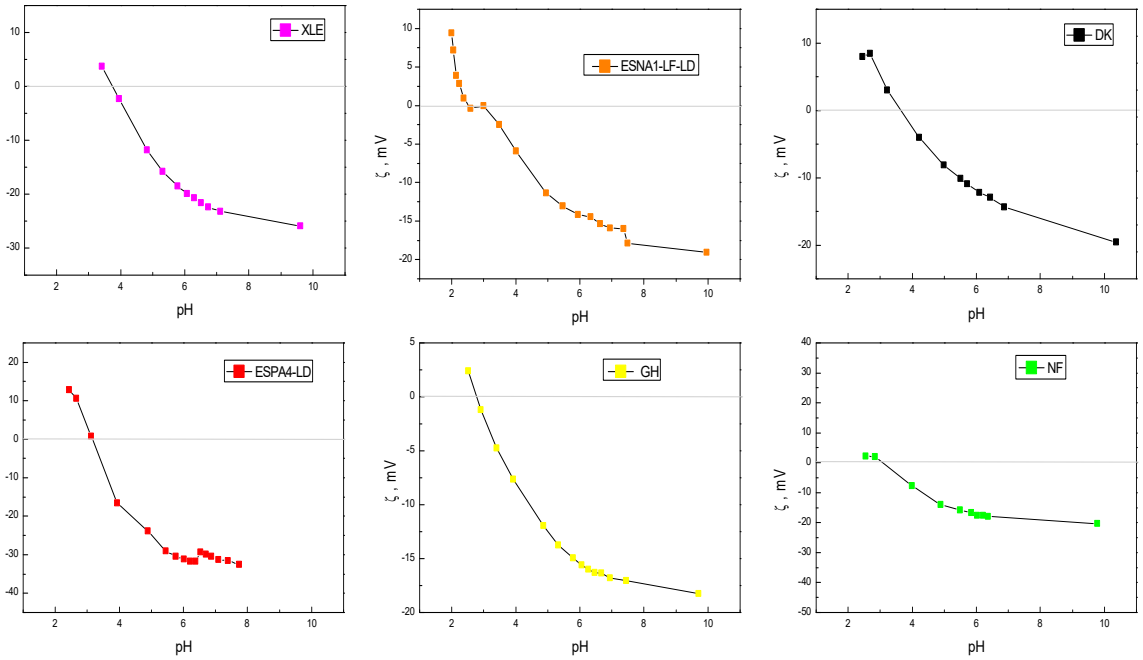

Figure 1. Zeta potential (ζ) of pure membranes as a function of pH.

The hydrophobicity/hydrophilicity of the surface of selected pristine membranes were determined using a goniometer, following the procedure described in Section 2.5. The obtained contact angle values are shown in Table 4. According to the literature, surfaces with a contact angle of less than 90° are classified as hydrophilic, while contact angles of less than 10° are defined as extremely hydrophilic, or superhydrophilic surfaces. In contrast, surfaces with a contact angle greater than 90° are considered hydrophobic, and contact angle values above 150° are characteristic of superhydrophobic surfaces [72].

Although all the membranes tested, which according to the standard classification (<90°) are hydrophilic, those with measured contact angles above 60° (ESNA1-LF-LD and XLE) can be described as relatively, or moderately hydrophobic, compared with the extremely hydrophilic membranes with smaller contact angles [60].

Before conducting the main experiments, the membranes were pressure treated at a pressure 20% higher than the working pressure and characterized using an inorganic salt (NaCl), in order to verify their nominal properties and confirm the correctness of the membranes themselves. The nominal properties of the membranes were determined by analyzing the flow of demineralized water (J) and the retention factor (R) of the NaCl solution, and the obtained values are shown in Table 5.

Table 5. Nominal properties of membranes.

Membranes						
Membrane type	**UF**	**NF**			**RO**	
	GH	**NF**	**DK**	**ESNA-1-LF-LD**	**XLE**	**ESPA4**
J, L/(m^2 h)	48.0	77.2	27.1	6.3	56.6	22.8
R (NaCl), %	48.9	37.8	58.1	90.2	75.8	94.2

As expected, RO membranes showed very high salt retention, particularly ESPA4, due to their compact structure and extremely small pores. NF membranes, which have larger pores, provide higher fluxes but lower salt retention than RO membranes. An exception is the NF

membrane ESNA-1-LF-LD, which nominally belongs to the NF group, but showed a very high retention factor (90.2%), comparable to RO membranes, with an extremely low flux (6.3 L/(m^2 h)). This behavior indicates an extremely dense structure and high selectivity within the NF category [54]; that is, this membrane is very likely a dense nanofiltration membrane. For the XLE membrane, which is a typical RO membrane, a retention of 75.8% was obtained, which is lower than expected, most likely due to the hydrodynamic conditions in that cell. Although the main role of UF membranes is the removal of suspended particles, colloids, viruses, bacteria, macromolecules, and suspended substances [54]. The GH membrane showed very high removal of NaCl, indicating that it lies at the boundary with nanofiltration membranes, as confirmed by its MWCO value of 2500 Da.

The obtained results confirm a clear gradation of membrane technologies: from highly selective RO membranes with minimal fluxes, through NF membranes with different compromises between flux and selectivity, to UF membranes that allow the passage of salt, but effectively remove larger particles and macromolecules [54].

3.2. Removal of Individual Anthelmintics, Neonicotinoid Insecticides, and Their Mixtures

After testing the nominal properties of the membranes, further research aimed to evaluate their effectiveness in removing selected antiparasitics (albendazole—ALB, febantel—FEB, mebendazole—MEB) and neonicotinoids (acetamiprid—ACE, clothianidin—CLO, thiacloprid—TIA) using different membrane processes. Special emphasis was placed on determining the retention factor and identifying the separation mechanisms of these compounds, using six membranes representing UF, NF, and RO.

The high efficiency of membrane processes in removing xenobiotics requires the simultaneous achievement of a high flow rate and a high retention factor. Retention factors for the tested anthelmintics are shown in Table 6, and for the pesticides in Table 7.

Table 6. Retention factors ALB, FEB, and MEB for tested RO/NF/UF membranes in demineralized and model water.

	***t*, h**	***R*, %**					
		GH	**NF**	**DK**	**ESNA-1-LF-LD**	**XLE**	**ESPA4**
				ALB			
DEMI WATER	1	74.7	81.4	87.9	>99.9	96.3	99.6
	2	57.0	69.7	78.0	99.3	93.8	98.6
	3	42.1	61.4	69.1	98.6	91.0	97.6
MODEL WATER	1	81.3	82.9	90.1	>99.9	96.3	>99.9
	2	76.6	81.9	86.9	>99.9	95.1	99.3
	3	78.0	83.7	87.6	>99.9	95.9	99.1
				FEB			
DEMI WATER	1	59.5	99.7	>99.9	99.7	99.9	99.9
	2	20.1	99.8	99.8	99.8	99.8	99.9
	3	15.1	99.6	99.7	99.8	99.7	99.6
MODEL WATER	1	42.5	99.7	99.1	99.2	99.4	>99.9
	2	9.5	99.7	99.1	99.4	98.7	>99.9
	3	8.6	99.7	99.1	99.5	98.4	>99.9
				MEB			
DEMI WATER	1	37.1	67.0	78.7	97.2	95.8	97.8
	2	32.1	64.2	74.2	94.5	95.5	97.1
	3	0.0	57.3	69.2	95.0	94.5	96.6
MODEL WATER	1	67.1	82.1	91.6	>99.9	98.2	>99.9
	2	69.6	82.4	88.3	99.3	97.9	99.5
	3	65.4	80.5	85.9	98.9	97.8	99.4

Table 7. Retention factors of ACE, CLO, and TIA for tested RO/NF/UF membranes in demineralized and model water.

	***t*, h**	***R*, %**					
		GH	**NF**	**DK**	**ESNA-1-LF-LD**	**XLE**	**ESPA4**
ACE							
DEMI WATER	1	10.9	45.7	59.2	97.7	78.2	95.4
	2	10.1	47.9	56.0	96.5	79.3	94.6
	3	9.2	45.7	56.9	95.9	80.5	94.3
MODEL WATER	1	8.8	43.2	61.9	97.1	84.9	97.8
	2	6.7	38.4	60.1	96.9	86.4	97.6
	3	2.2	39.4	56.5	97.1	89.0	97.6
CLO							
DEMI WATER	1	0.0	18.9	33.7	94.8	82.0	94.9
	2	1.1	20.7	35.7	95.6	84.9	94.3
	3	0.0	20.9	35.3	96.2	86.7	94.1
MODEL WATER	1	0.3	21.5	43.5	92.7	85.5	96.4
	2	0.4	18.2	41.2	92.5	87.1	95.6
	3	0.2	20.0	41.1	92.9	88.4	95.6
TIA							
DEMI WATER	1	2.7	27.8	45.6	97.9	79.8	96.4
	2	0.0	25.9	41.5	97.8	80.4	95.7
	3	1.2	27.7	42.8	97.8	82.2	95.7
MODEL WATER	1	5.5	26.3	49.4	97.0	83.5	97.2
	2	6.6	24.1	46.9	96.7	84.9	97.0
	3	6.8	23.8	44.6	96.8	86.9	96.9

RO membranes (XLE, ESPA4) and the dense NF membrane (ESNA1-LF-LD) showed almost complete removal of all tested anthelmintics. These results are consistent with their structural properties, primarily their lowest MWCO values, which indicates that the main removal mechanism is size exclusion, or the sieving effect. Considering the comparison between the molecular weights of the components and the MWCO limit values of the membranes, it is clear that the sieving effect dominates over other removal mechanisms. Nanofiltration membranes (DK and NF) showed the expected removal. This result is expected given the significantly higher fluxes of the NF membrane, larger contact angle, lower zeta potential, and higher MWCO [60]. The ultrafiltration membrane GH, in line with its highest MWCO, lowest surface charge, and medium hydrophilicity, showed the lowest removal efficiency. Nevertheless, it is interesting that the retention of ALB on the GH membrane was comparable to that on the NF membrane. This phenomenon can be explained by the pronounced hydrophobicity of ALB (higher $\log K_{O/W}$ compared with other anthelmintics), which increases its tendency to adsorb onto the membrane surface and thereby apparently increases retention, despite the higher MWCO.

Within the group of antiparasitics tested, ALB was the most hydrophobic compound (Table 1). In addition, ALB is also the smallest molecule among those tested with a molar mass of 265.33 g/mol. The high hydrophobicity of ALB enhances its interactions with the membrane surface, while the higher MWCO and weaker hydrophobic interactions explain the variable efficiency of NF membranes [73]. According to the literature, compounds with a $\log K_{O/W}$ value greater than 2 (such as ALB and MEB) are considered hydrophobic and tend to adsorb both on the membrane surface and within its structure, which can result in higher removal than expected. Consequently, adsorbed components can diffuse through the membrane, especially in the case of NF membranes, and such behavior results in lower retention factors than would be expected [60]. This is also evident in the results for ALB and MEB, where retention decreases over time. In contrast to ALB, FEB stands out with the highest molar mass (446.48 g/mol) and the lowest $\log K_{O/W}$ value. The molar mass of FEB is higher than the MWCO value of all membranes, except for the GH membrane, which

is also reflected in the results (Table 6). Almost complete retention of FEB was achieved with all NF and RO membranes, which is in accordance with the literature [63], while the GH membrane shows extremely low removal values. These results are in accordance with the literature, which emphasizes that pore size dominates the retention mechanism, while hydrophilicity reduces the tendency to adsorb on the membrane surface [74]. Comparing the removal of FEB and ALB with the GH membrane clearly shows the influence of molecular hydrophobicity on removal. Based on the physico-chemical properties (Table 1), MEB is classified as a hydrophobic compound and shows removal patterns comparable to those determined for ALB [75]. Overall, the results confirm that the main removal mechanism for membranes with lower MWCO is size exclusion. Additionally, depending on the properties of the compound (hydrophobicity) and the membrane (hydrophilicity/hydrophobicity, zeta potential), it can be assumed that electrostatic repulsion and adsorption further affect the total removal of the tested components.

The RO membrane (ESPA4) and the dense NF membrane (ESNA1-LF-LD) showed almost complete removal of all tested pesticides (Table 7). These results are consistent with the low MWCO values of these membranes, which confirms that the main retention mechanism is again size exclusion. Although RO membranes generally show very high pesticide removal, it was observed that the XLE membrane achieved slightly lower retention compared with the previously mentioned RO membranes. This result can be explained primarily by the hydraulic properties of the membrane itself. The XLE is designed as an RO membrane with higher water permeability, which means that it achieves a higher flow rate under the same operating conditions. The increased flow of the solution through the membrane leads to more pronounced concentration polarization on its surface, i.e., the accumulation of pesticides in the boundary layer. Consequently, this can result in lower retention compared with lower flux membranes.

Given that the molar masses of ACE, TIA, and CLO are lower than the MWCO limit values for UF and most NF membranes, it is expected that the membranes with the smallest pores (RO and dense NF) will achieve the highest efficiency.

By comparing the results for the tested compounds, no significant differences in retention were observed, which is in accordance with their similar molar masses and hydrophilic properties. The slightly lower removal of CLO compared with ACE and TIA present in NF membranes can be related to its greater hydrophilicity and higher solubility in water, which increases the probability of passing through the membrane. On the other hand, the high retention of ACE and TIA on dense NF and RO membranes further confirms that MWCO and size exclusion dominate over other removal mechanisms.

The retention factors, after 3 h treatment, obtained for the six-component mixture dissolved in demineralized water are presented in Table 8.

After 3 h of filtration of the six-component mixture, the relative performance of the NF and RO membranes varied with the compound and water matrix (Table 8). In demineralized water, ESPA4 showed higher rejection than ESNA1-LF-LD for five of the six compounds, and XLE gave the highest MEB rejection (>99.9%). In model water, ESNA1-LF-LD and ESPA4 showed similar rejection values, with ESNA1-LF-LD giving the highest reported rejection for all six compounds. The ultrafiltration membrane GH exhibited negligible removal of the investigated neonicotinoid insecticides, while only moderate rejection was achieved for benzimidazole anthelmintics. Such behavior is expected considering the large pore size of UF membranes, where size exclusion is insufficient to retain relatively small organic molecules. Consequently, the separation of these compounds is governed predominantly by adsorption phenomena rather than steric hindrance, resulting in low overall rejection. A substantial improvement in removal efficiency was observed for nanofiltration membranes. Although NF and DK membranes retained benzimidazole anthelmintics more

efficiently than neonicotinoid insecticides, the dense NF membrane ESNA1-LF-LD achieved rejection values above 87% for all investigated compounds. The superior performance of this membrane can be attributed to its MWCO values and denser selective layer. The reverse osmosis membranes XLE and ESPA4 exhibited the highest separation efficiency, providing rejection values exceeding 90% for almost all compounds, whereas febantel was completely retained by both membranes. Owing to their highly compact polyamide selective layer, the transport of dissolved organic molecules through RO membranes is substantially restricted, resulting in consistently high rejection irrespective of compound class.

Table 8. Retention factors of the tested membranes for xenobiotics, t = 3 h.

	***R*, %**					
	CLO	**ACE**	**TIA**	**MEB**	**ALB**	**FEB**
			DEMI WATER			
GH	0.0	0.0	0.0	48.8	27.1	50.9
NF	14.3	27.1	18.7	75.7	53.9	>99.9
DK	32.8	53.9	43.4	85.8	58.1	>99.9
ESNA-1-LF	87.9	88.0	87.9	92.6	90.1	>99.9
XLE	90.9	91.2	89.8	>99.9	92.5	>99.9
ESPA4	94.5	94.5	94.8	94.7	94.8	>99.9
			MODEL WATER			
GH	0.4	0.5	0.0	68.9	67.6	59.5
NF	12.3	24.8	15.9	81.8	73.9	97.2
DK	41.5	62.1	51.0	88.0	80.6	96.6
ESNA-1-LF	94.7	94.9	94.4	97.4	97.9	>99.9
XLE	91.2	91.4	90.1	97.3	97.1	98.2
ESPA4	93.0	93.0	92.9	96.6	97.3	97.8

Comparison of the results obtained for the six-component mixture with those observed for individual compounds indicates that the presence of multiple xenobiotics did not substantially alter the overall separation trend. Nevertheless, slight variations in retention factors suggest that competitive interactions among dissolved compounds may occur during membrane treatment. In multicomponent systems, xenobiotics compete for adsorption sites on the membrane surface and within the active polyamide layer, while simultaneous concentration polarization may additionally influence mass transport. Consequently, retention in complex mixtures cannot always be predicted solely from the behavior of individual compounds. Regardless of the membrane applied, benzimidazole anthelmintics were generally retained more efficiently than neonicotinoid insecticides. This behavior is consistent with their larger molecular dimensions and, particularly for ALB and MEB, with higher hydrophobicity, which favours adsorption onto the membrane surface. In contrast, neonicotinoid insecticides are smaller and generally more hydrophilic molecules, allowing easier transport through membranes with larger pore sizes. Similar observations have been reported in previous studies investigating the membrane removal of veterinary pharmaceuticals and pesticides, where compound size, molecular configuration and membrane physico-chemical properties were identified as the principal factors governing separation efficiency [61,62].

The retention factors obtained in model water were generally higher than those observed in demineralized water. This finding indicates that water matrix composition significantly influences membrane separation performance. The presence of dissolved inorganic ions increases ionic strength, which may alter membrane surface charge as well as the speciation of ionisable xenobiotics [62]. Such changes reduce electrostatic repulsion between the membrane and dissolved compounds and may enhance concentration polarization, leading to improved apparent rejection.

ESNA1-LF-LD, XLE, and ESPA4 were among the most effective membranes in both water matrices. Particularly high retention was observed for FEB, which was almost com-

pletely removed by all dense NF and RO membranes. These results demonstrate that pressure-driven membrane processes remain highly effective even under more realistic water conditions, where dissolved salts and other constituents may interfere with membrane transport phenomena.

Comparison of the retention factors obtained for individual xenobiotics and the six-component mixture revealed that the overall separation behavior remained largely unchanged, although slightly lower rejection values were observed for several compounds in the multicomponent system. After 3 h in demineralized water, ALB rejection by GH decreased from 42.1% in the single compound experiment to 27.1% in the mixture, whereas MEB rejection increased from 0.0% to 48.8% (Tables 6 and 8). Among neonicotinoid insecticides, ACE and TIA also exhibited slightly lower retention in the mixture, particularly on GH and NF membranes, while the differences became negligible for dense NF and RO membranes. These observations suggest that the presence of multiple dissolved xenobiotics may influence membrane separation through competition for adsorption sites and changes in mass transport near the membrane surface. Such effects become evident primarily in membranes with larger pores, where adsorption contributes significantly to overall retention. Conversely, in dense NF and RO membranes, steric exclusion remains the dominant removal mechanism, making retention considerably less sensitive to the presence of additional compounds.

3.3. FTIR Analysis

Adsorption of anthelmintics onto the polyamide layer of membranes has been confirmed by FTIR analysis, highlighting the importance of compound–membrane interactions in the overall removal process [54,60]. After the xenobiotic removal tests and drying of the used membranes, FTIR analysis was performed to examine possible interactions and adsorption of xenobiotics on the membrane surface. The results obtained are shown in Figures 2 and 3.

By analyzing the FTIR spectra of the membranes after removing ALB, MEB, and FEB, characteristic bands were observed that confirm the adsorption of the investigated antiparasitics on the membrane polymer matrix (Figure 2). Aromatic signals in the region 730–805 cm^{-1} and bands in the amide regions are common to all compounds: amide I (≈1648–1622 cm^{-1}) and amide II (≈1523 cm^{-1}). These bands, together with the bands of the amide III region (≈1195–1275 cm^{-1}), indicate the interaction of the investigated molecules with the polyamide membrane.

ALB shows the most pronounced changes in the spectrum (Figure 2). Its carbonyl groups give clear bands around 1714 cm^{-1} and 1746 cm^{-1}, indicating the existence of two different microenvironments of carbonyl groups. In model solutions, a slight shift in the carbonyl band towards lower wavenumbers (1719 → 1713 cm^{-1}) was frequently observed, which is interpreted as stronger H-bonding and the influence of ionic strength. In addition, ALB shows characteristic bands related to methyl and methylene groups: $-CH_3$ bending in the region of 800–1000 cm^{-1}, and $-CH_2$ bending in the aliphatic part of the molecule at 762 cm^{-1} and 790 cm^{-1}. In the region of 1194–1269 cm^{-1}, bands attributed to $C(sp^2)-O-C(sp^3)$ stretching and C–O–C deformations were observed, which further confirms the presence of carbamate centers [60].

In MEB, aromatic and carbonyl bands are also dominant, but a more stable spectroscopic signature is observed between demineralized and model water. The double carbonyl bands present in most of the membranes confirm different types of H-bonding, while the increased hydrophobicity of the compound additionally explains its pronounced adsorption on the polyamide layer. In the MEB spectrum (Figure 2), a new carbonyl band was observed at 1735 cm^{-1}, corresponding to a new carbonyl group [60]. In the region around

1647 cm^{-1}, a band was observed that can be attributed to the vibrations of the amide C=O bonds of primary and secondary amides, with a possible contribution from alkenyl C=C stretching [60,76,77]. In the lower range of the spectrum, between 800 and 1000 cm^{-1}, the bending of methyl ($-CH_3$) groups is present, while at 762 cm^{-1} the characteristic bending of methylene ($-CH_2$) groups appears [60].

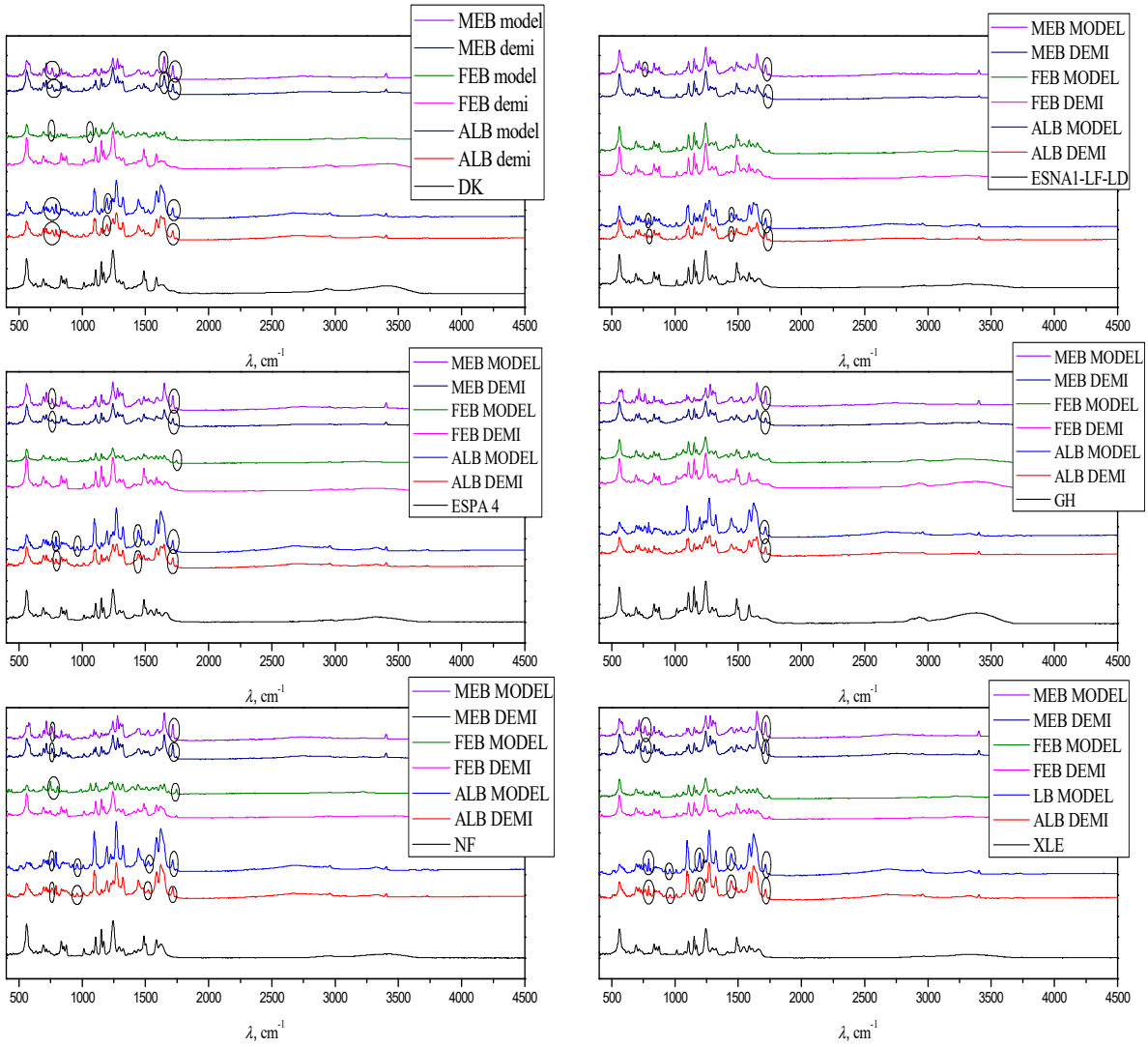

Figure 2. FTIR spectra of membranes before and after treatment of individual anthelmintic solutions prepared in demineralized and model water.

FEB shows the weakest traces in demineralized water (often without a clear carbonyl band), while pronounced aromatic and carbamate bands appear in model solutions. This indicates a stronger matrix effect and enhanced adsorption under conditions of higher ionic strength. Characteristic bands at 1746 cm^{-1} were observed, corresponding to carbamate-type carbonyl groups (Figure 2).

Overall, the FTIR results confirm that the adsorption of the investigated antiparasitics takes place via aromatic and carbamate centers, with the influence of H-bond formation and hydrophobic interactions being pronounced for ALB and MEB, while for FEB the influence of the matrix and ionic strength is dominant. These findings further support the results on separation efficiency, where ALB showed the weakest and FEB the most pronounced separation in membrane processes.

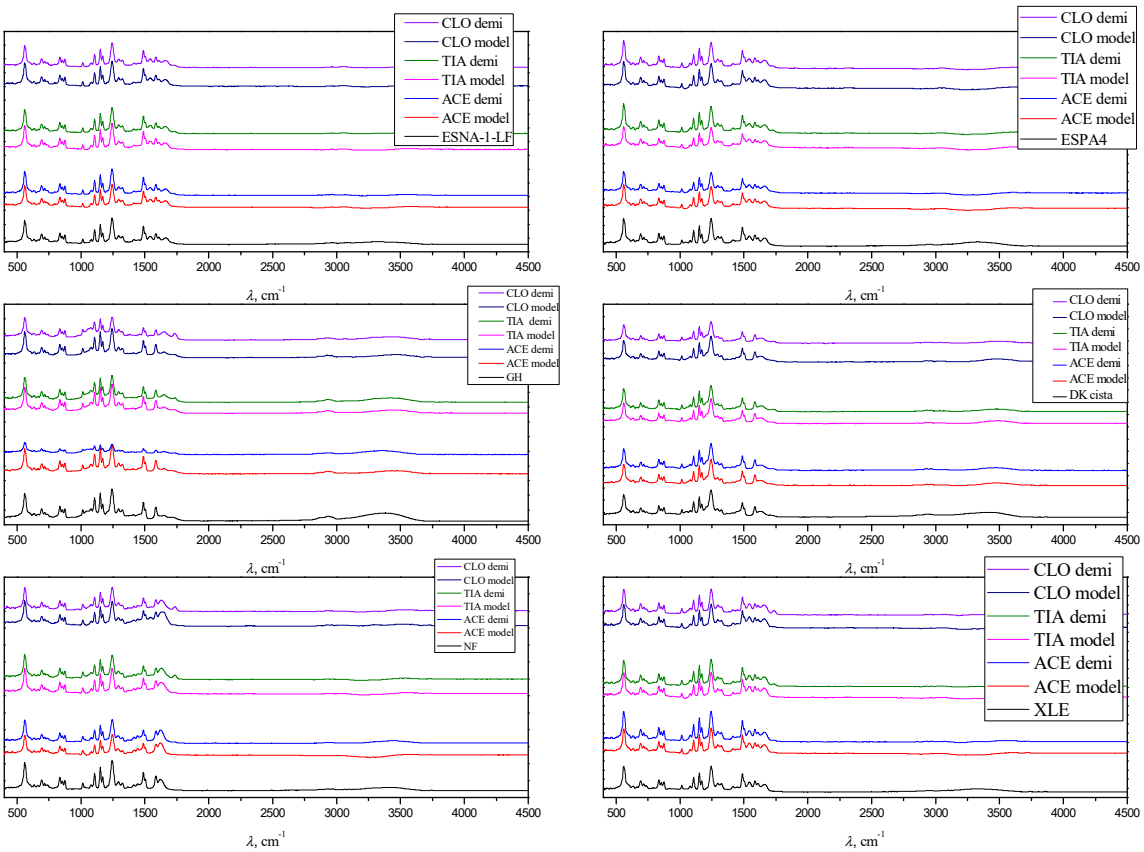

Figure 3. FTIR spectra of membranes before and after treatment of individual neonicotinoid solutions prepared in demineralized and model water.

FTIR analysis of the membranes after treatment of the six component mixture revealed spectral changes consistent with those observed following treatment of individual compounds (Figure 4). As discussed previously, the appearance of new absorption bands was detected exclusively after the treatment with benzimidazole anthelmintics, whereas no additional bands were observed following the treatment of neonicotinoid insecticides. The same spectral pattern was observed after treatment of the multicomponent mixture (Figure 4), indicating that interactions between the membrane surface and the investigated xenobiotics were predominantly governed by the presence of benzimidazole derivatives. Furthermore, no significant differences were observed between the FTIR spectra of membranes used for treatment of the six-component mixture prepared in demineralized and model water (Figure 4). This indicates that the water matrix had no measurable influence on the chemical interactions occurring at the membrane surface, suggesting that the adsorption behavior of the investigated xenobiotics remained largely unchanged under the applied experimental conditions.

The partition coefficient ($\log K_{O/W}$) of the target compounds plays a significant role in determining their affinity for membrane materials and thus their retention behavior [73]. Because pesticides have lower $\log K_{O/W}$ values and higher solubility in water then anthelmintics, they are not expected to be adsorbed to any significant extent on the membrane surface. Accordingly, FTIR analysis of the membranes after pesticide removal did not reveal any new bands indicating the presence of adsorbed compounds. This confirms that the removal of pesticides in this procedure is based primarily on a size exclusion mechanism rather than on adsorption processes.

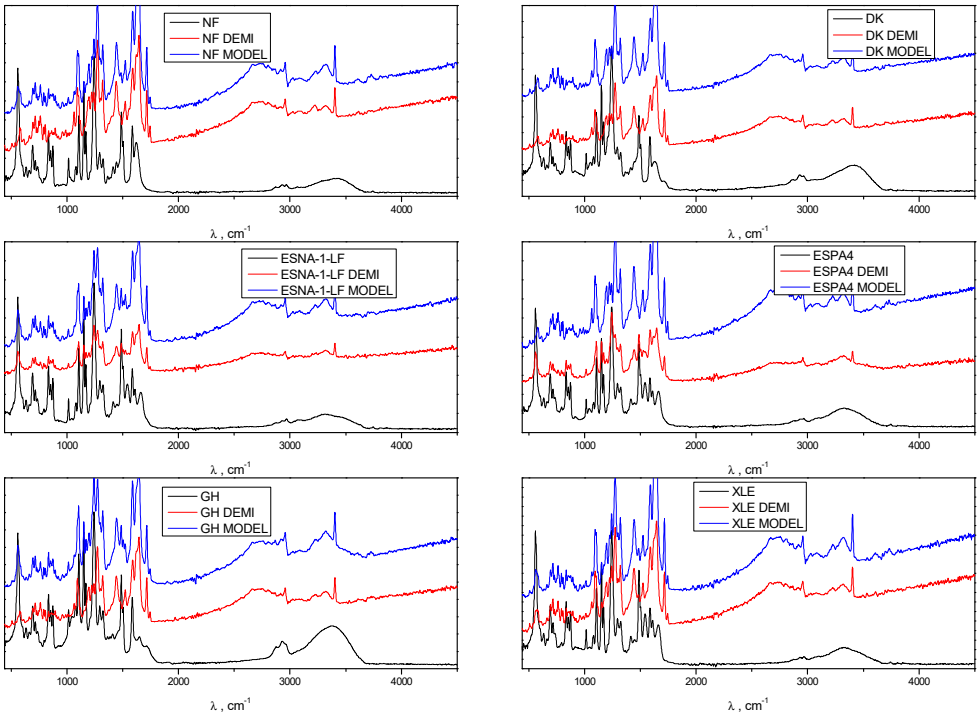

Figure 4. FTIR spectra of membranes after treatment with a six component mixture.

3.4. Ecotoxicity

Monitoring ecotoxicity after membrane treatment is an important part of assessing process efficiency because analytically determined concentrations of target xenobiotics do not necessarily reflect their overall biological effects. Even after reducing the concentration of pollutants in the permeate, compounds or their transformation products may remain that retain a certain degree of toxicity. Therefore, the *Vibrio fischeri* inhibition test was conducted to determine the extent to which membrane processes reduce not only the concentration of the tested xenobiotics, but also their potential harmful effects on aquatic organisms. The initial solution of each compound was analyzed before membrane treatment and served as a reference value for comparison with the permeates obtained by filtration through the tested UF, NF and RO membranes.

Of the tested antiparasitics, only the initial solution of MEB in demineralized water showed measurable acute ecotoxicity towards *Vibrio fischeri*, with maximum inhibition of approximately 29%. After membrane treatment, inhibition was reduced to 0% for all tested membranes (Table 9), indicating that MEB removal was sufficient to eliminate its inhibitory effect completely. This result confirms that membrane separation effectively reduces the biological activity of this compound and that the reduction in its concentration is directly reflected in the reduction in the ecotoxicity of the permeate.

Unlike MEB, ALB, and FEB, no inhibitory effect was observed either before or after membrane treatment, regardless of the type of membrane applied or the composition of the aqueous matrix. These results suggest that, at the tested concentration of 10 mg/L, these compounds do not exhibit acute toxicity towards the bacterium *Vibrio fischeri*. Consequently, although the membrane processes achieved very high retention factors for these compounds, especially with nanofiltration and reverse osmosis membranes, their removal did not lead to an additional decrease in inhibition, as inhibition was absent even in the initial solutions.

Table 9. Inhibitions of solutions after treatment with the membrane process.

Sample	*INHB*, %						
	10 mg/L	**GH**	**NF**	**DK**	**ESNA-1-LF-LD**	**XLE**	**ESPA4**
ALB DEMI	0.0	0.0	0.0	0.0	0.0	0.0	0.0
ALB MODEL	0.0	0.0	0.0	0.0	0.0	0.0	0.0
FEB DEMI	0.0	0.0	0.0	0.0	0.0	0.0	0.0
FEB MODEL	0.0	0.0	0.0	0.0	0.0	0.0	0.0
MEB DEMI	29.9	0.0	0.0	0.0	0.0	0.0	0.0
MEB MODEL	0.0	0.0	0.0	0.0	0.0	0.0	0.0
ACE DEMI	39.9	20.2	18.7	6.1	0.0	0.0	0.0
ACE MODEL	32.2	25.3	3.0	0.0	0.0	0.0	0.0
CLO DEMI	15.1	10.7	0.0	0.0	0.0	0.0	0.0
CLO MODEL	18.9	14.0	0.0	0.0	0.0	0.0	0.0
TIA DEMI	35.3	23.5	4.3	0.0	0.0	0.0	0.0
TIA MODEL	29.6	20.2	1.0	0.0	0.0	0.0	0.0

In contrast to the antiparasitics, all three tested neonicotinoid pesticides showed pronounced initial ecotoxicity. The highest inhibitory effect was recorded for ACE, whose initial inhibition in demineralized water was 39.9%, while CLO and TIA showed lower inhibition values. After membrane treatment, a clear trend of ecotoxicity reduction with increasing membrane separation efficiency was observed. With the ultrafiltration membrane, GH, inhibition decreased but remained relatively high, which is consistent with the very low retention factors obtained for this membrane. The NF nanofiltration membrane further reduced inhibition, while with the dense nanofiltration membrane ESNA-1-LF-LD and both reverse osmosis membranes (XLE and ESPA4) inhibition was completely removed. These results confirm that the reduction in ecotoxicity is directly related to an increase in the retention factor; that is, more efficient membranes produce permeate with a lower biological effect.

A similar pattern was observed with model water. Although the initial inhibition of the pesticides remained pronounced, after membrane treatment the inhibition values were equal to or lower than those in demineralized water. The NF membrane is particularly noteworthy, as for acetamiprid the inhibition was reduced from 25.3% to only 3.0%, while with the other denser membranes inhibition was no longer detected. The results, consistent with the previously determined higher retention factors in model water, confirm that improved membrane separation efficiency directly contributes to reducing the ecotoxicity of the permeate.

Overall, the ecotoxicity results correlate well with the chemical analyzes and the obtained retention factors. The membranes that showed the highest xenobiotic removal efficiency, namely ESNA-1-LF-LD, XLE and ESPA4, produced permeate without measurable acute toxicity to *Vibrio fischeri*. In contrast, the lower selectivity membranes, especially the GH ultrafiltration membrane, showed a higher residual inhibition due to the passage of a larger proportion of the tested compounds into the permeate.

The ecotoxicity test results for a mixture of six xenobiotics against *Vibrio fischeri* showed that the initial solution prepared in demineralized water (Figure 5) was significantly less toxic than the same mixture prepared in model water (Figure 6). At the highest volume fraction of the sample, the inhibition of bioluminescence was 86.8% for model water, and 63.6% for demineralized water.

Since model water did not cause an increase in the toxicity of individual compounds during testing, it can be assumed that the increased inhibition results from interactions between components within the multicomponent mixture.

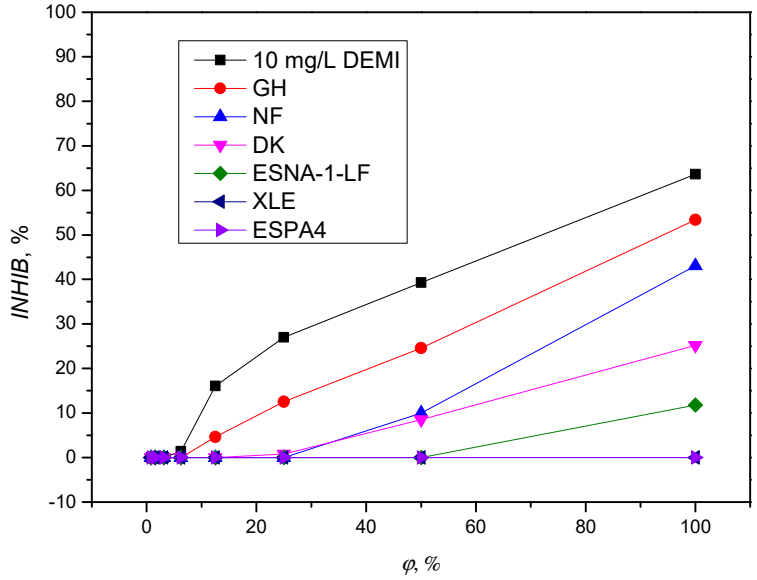

Figure 5. Inhibition of *Vibrio fischeri* depending on the volume fraction of the xenobiotic mixture solution during membrane treatment in demineralized water.

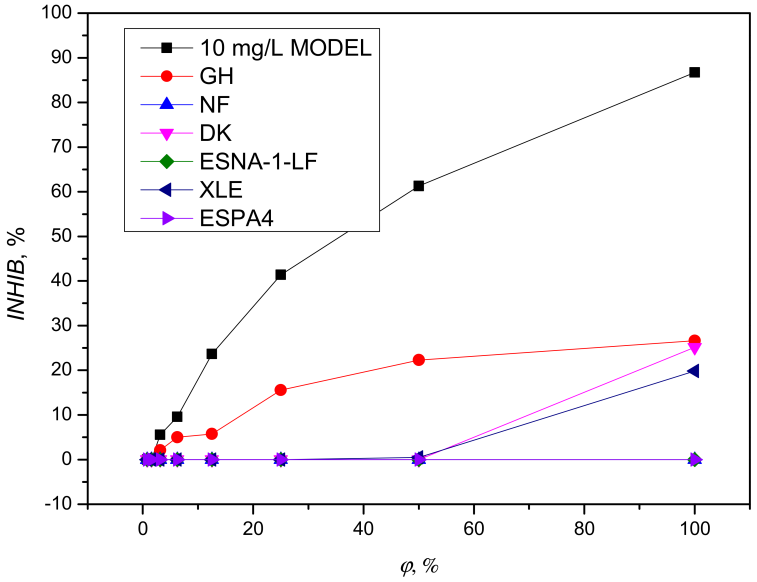

Figure 6. Inhibition of *Vibrio fischeri* depending on the volume fraction of the solution of the xenobiotic mixture during membrane treatment of the same in a model solution.

In mixtures of organic pollutants, the total toxicity is often not equal to the sum of the effects of the individual components [78]. Depending on their mutual interactions, additive, synergistic or antagonistic effects may occur [79]. Such interactions are particularly pronounced in mixtures of pesticides and veterinary drugs, because the compounds can affect different physiological processes or mutually influence their bioavailability and uptake into the body [78].

The higher toxicity of the mixture in model water can be explained by the influence of the matrix on the physico-chemical properties of individual compounds. The presence of inorganic ions and different ionic strengths can change the degree of ionization, solubility, and distribution of individual anthelmintics and neonicotinoid insecticides and thus increase their biological effect. Although model water itself did not show an increase in the toxicity

of individual compounds, its composition may favour the development of additive or synergistic effects within the multicomponent mixture.

After membrane treatment, a significant reduction in bioluminescence inhibition was observed for all tested membranes, with the efficiency depending on membrane properties. The greatest reduction in toxicity was achieved with the XLE and ESPA4 membranes, for which inhibition was not recorded even at the highest volume fraction of permeate, indicating almost complete removal of the toxic components of the mixture. The ESNA-1-LF membrane also showed very good efficiency, while the GH, NF, and DK membranes resulted in a partial reduction in inhibition. This trend is in line with expectations, as membranes with higher densities and smaller effective pore diameters achieve higher retention of organic micropollutants.

In multicomponent systems, different compounds compete with each other during transport through the membrane, and selective removal of individual components can change the composition of the permeate and thus its overall ecotoxicological effect. Therefore, the acute toxicity of the permeate may not be directly correlated with the total concentration of all analyzed compounds, but primarily depends on the concentration of those components that contribute most to the biological response.

4. Conclusions

This study demonstrated the strong potential of pressure-driven membrane processes for removing veterinary anthelmintics, neonicotinoid insecticides, and their mixtures from water. Membrane performance depended strongly on membrane characteristics, with removal efficiency consistently increasing from ultrafiltration to nanofiltration and reverse osmosis. Dense NF and RO membranes achieved the highest rejection efficiencies for all investigated compounds, whereas UF membranes showed limited removal, particularly for neonicotinoid insecticides.

The results confirmed that membrane retention is governed by a combination of steric exclusion, adsorption, and electrostatic interactions. Compound physico-chemical properties, especially molecular size, hydrophobicity, and molecular weight, significantly influenced removal efficiency, while water matrix composition also affected membrane performance. In general, higher retention was achieved in model water, indicating that dissolved inorganic constituents modify membrane–solute interactions.

FTIR analysis confirmed adsorption of benzimidazole anthelmintics onto membrane surfaces, whereas no significant adsorption of neonicotinoid insecticides was observed. Similar spectral features obtained after membrane treatment of the six-component mixture suggest that membrane–solute interactions remained dominated by benzimidazole derivatives irrespective of solution composition.

Ecotoxicity assessment showed that membrane treatment substantially reduced the biological effects of the investigated xenobiotics, particularly after NF and RO. The good agreement between chemical analysis and ecotoxicological response confirms that pressure-driven membrane processes can reduce both contaminant concentrations and their associated environmental risks.

Overall, this study provides new insight into the simultaneous removal of veterinary pharmaceuticals and neonicotinoid insecticides under different water matrix conditions and demonstrates the importance of integrating chemical, spectroscopic, and ecotoxicological analyses when evaluating advanced membrane treatment technologies. These findings improve understanding of membrane separation mechanisms and support the application of pressure-driven membrane processes for treating waters contaminated with complex mixtures of organic micropollutants.

Supplementary Materials: The following supporting information can be downloaded at https://www.mdpi.com/article/10.3390/membranes16110395/s1: Table S1: List of chemicals used during experiments; Table S2: Composition of the model solution; Table S3: Characteristics of the tested commercial membranes.

Author Contributions: Investigation, writing—original draft, formal analysis, validation, B.B.V.; Investigation, formal toxicity analysis, P.M.; Investigation, formal toxicity analysis, V.S.; Investigation (analytical part), validation, writing—review and editing, D.A.; Conceptualization, investigation, methodology, writing—review and editing, D.D. All authors have read and agreed to the published version of the manuscript.

Funding: This research was funded by the NATO Science for Peace and Security Programme under grant id. G6087.

Institutional Review Board Statement: Not applicable.

Informed Consent Statement: Not applicable.

Data Availability Statement: The data presented in this study are available on request from the corresponding author.

Conflicts of Interest: The authors declare no conflicts of interest.

References

1. Štefanac, T.; Grgas, D.; Landeka Dragičević, T. Xenobiotics—Division and Methods of Detection: A Review. *J. Xenobiot.* **2021**, *11*, 130–141. [CrossRef] [PubMed]
2. Donner, E.; Eriksson, E.; Holten-Lützhøft, H.-C.; Scholes, L.; Revitt, M.; Ledin, A. Identifying and Classifying the Sources and Uses of Xenobiotics in Urban Environments. In *Xenobiotics in the Urban Water Cycle*; Fatta-Kassinos, D., Bester, K., Kümmerer, K., Eds.; Springer: Dordrecht, The Netherlands, 2009; pp. 27–50.
3. Thakur, I.S. Xenobiotics: Pollutants and their degradation-methane, benzene, pesticides, bioabsorption of metals. In *Environmental Microbiology*; NISCAIR: New Delhi, India, 2008; pp. 3–6.
4. Patterson, A.D.; Gonzalez, F.J.; Idle, J.R. Xenobiotic metabolism—A view through the metabolometer. *Chem. Res. Toxicol.* **2010**, *23*, 851–860. [CrossRef] [PubMed]
5. Singh, M.; Chandra Mishra, R.; Shah, I.; Wadhwa, V.; Mor, V. Xenobiotics: Sources, Pathways, Degradation, and Risk Associatedwith Major Emphasis on Pharmaceutical Compounds. In *Xenobiotics in Urban Ecosystems: Sources, Distribution and Health Impacts*; Singh, R., Singh, P., Tripathi, S., Chandra, K.K., Bhadouria, R., Eds.; Springer International Publishing: Dordrecht, The Netherlands, 2023; Volume 1, pp. 96–115.
6. Fatta-Kassinos, D.; Bester, K.; Kümmerer, K. *Xenobiotics in the Urban Water Cycle: Mass Flows, environmental Processes, Mitigation and Treatment Strategies*; Springer Science & Business Media: Dordrecht, The Netherlands, 2010; Volume 16, pp. 4–19, 388–396.
7. Guptaa, S.K.; Singh, B.; Mungray, A.K.; Bharti, R.; Nema, A.K.; Pant, K.K.; Mulla, I.S. Bioelectrochemical technologies for removal of xenobiotics from wastewater. *Sustain. Energy Technol. Assess.* **2022**, *49*, 101652. [CrossRef]
8. Pedersen, A.B.; Fenton, A. The role of antiparasite treatment experiments in assessing the impact of parasites on wildlife. *Trends Parasitol.* **2015**, *31*, 200–211. [CrossRef] [PubMed]
9. Cooper, K.M.; Whelan, M.; Kennedy, D.G.; Cannavan, G.T.A.; Boon, P.E.; Wapperom, D.; Danaher, M. Anthelmintic drug residues in beef: UPLC-MS/MS method validation, European retail beef survey, and associated exposure and risk assessments. *Food Addit. Contam.* **2012**, *29*, 746–760. [CrossRef] [PubMed]
10. Crosby, N.T. *Determination of Veterinary Residues in Food*; Woodhead Publishing Limited: Cambridge, UK; Volume 1, pp. 66–78.
11. Weller, P.F.; Liu, L.X. Antiparasitic drugs. *N. Engl. J. Med.* **1996**, *334*, 1178–1184. [CrossRef] [PubMed]
12. Page, S.W. Antiparasitic drugs. In *Small Animal Clinical Pharmacology*; Maddison, J.E., Page, S.W., Church, D.B., Eds.; Saunders Elsevier: Edinburgh, UK, 2008; Volume 2, pp. 198–208. [CrossRef]
13. Kuhlmann, F.M.; Fleckenstein, J.M. Antiprasitic Agents. In *Infectious Diseases*; Cohen, J., Powderly, W.G., Opal, S.M., Eds.; Elsevier: Philadelphia, PA, USA, 2017; Volume 4, pp. 1345–1371.
14. al Jalali, V.; Zeitlinger, M. Systemic and Target-Site Pharmacokinetics of Antiparasitic Agents. *Clin. Pharmacokinet.* **2020**, *59*, 827–840. [CrossRef] [PubMed]
15. Papich, M.G. *Saunders Handbook of Veterinary Drugs*; Elsevier: Philadelphia, PA, USA, 2016; Volume 5, pp. 312–313, 478–479.
16. Li, Y.; Gan, Z.; Liu, Y.; Chen, S.; Su, S.; Ding, S.; Tran, N.H.; Chen, X.; Long, Z. Determination of 19 anthelmintics in environmental water and sediment using an optimized PLE and SPE method coupled with UHPLC-MS/MS. *Sci. Total Environ.* **2020**, *719*, 137516. [CrossRef] [PubMed]

17. Sim, W.J.; Kim, H.Y.; Choi, S.D.; Kwon, J.H.; Oh, J.E. Evaluation of pharmaceuticals and personal care products with emphasis on anthelmintics in human sanitary waste, sewage, hospital wastewater, livestock wastewater and receiving water. *J. Hazard. Mater. 248–249*, 219–227. [CrossRef] [PubMed]
18. Dolar, D.; Pelko, S.; Košutić, K.; Horvat, A.J.M. Removal of anthelmintic drugs and their photodegradation products from water with RO/NF membranes. *Process Saf. Environ. Prot.* **2012**, *90*, 147–152. [CrossRef]
19. Kwarciak-Kozlowska, A. 7-Removal of Pharmaceuticals and Personal Care Products by Ozonation, Advance Oxidation Processes, and Membrane Separation. In *Pharmaceuticals and Personal Care Products: Waste Management and Treatment Technology: Emerging Contaminants and Micro Pollutants*; Prasad, M.N.V., Vithanage, M., Kapley, A., Eds.; Elsevier Inc.: Amsterdam, The Netherlands, 2019; Volume 1, pp. 151–171. [CrossRef]
20. Rizzo, L.; Malato, S.; Antakyali, D.; Beretsou, V.G.; Đolić, M.B.; Gernjak, W.; Heath, E.; Ivancev-Tumbas, I.; Karaolia, P.; Lado Ribeiro, A.R.; et al. Consolidated vs new advanced treatment methods for the removal of contaminants of emerging concern from urban wastewater. *Sci. Total Environ.* **2019**, *655*, 986–1008. [CrossRef] [PubMed]
21. Wang, J.; Wang, S. Removal of pharmaceuticals and personal care products (PPCPs) from wastewater: A review. *J. Environ. Manag.* **2016**, *182*, 620–640. [CrossRef] [PubMed]
22. Klatte, S.; Schaefer, H.C.; Hempel, M. Pharmaceuticals in the environment—A short review on options to minimize the exposure of humans, animals and ecosystems. *Sustain. Chem. Pharm.* **2017**, *5*, 61–66. [CrossRef]
23. Horvat, A.J.M.; Babić, S.; Pavlović, D.M.; Ašperger, D.; Pelko, S.; Kaštelan-Macan, M.; Mance, A.D. Analysis, occurrence and fate of anthelmintics and their transformation products in the environment. *TrAC* **2012**, *31*, 61–84. [CrossRef]
24. Lian, Z.; Liang, Z.; Wang, J. Selective extraction and concentration of mebendazole in seawater samples using molecularly imprinted polymer as sorbent. *Mar. Pollut. Bull.* **2015**, *91*, 96–101. [CrossRef] [PubMed]
25. Zajíčková, M.; Nguyen, L.T.; Skálová, L.; Raisová Stuchlíková, L.; Matoušková, P. Anthelmintics in the future: Current trends in the discovery and development of new drugs against gastrointestinal nematodes. *Drug Discov.* **2020**, *25*, 430–437. [CrossRef] [PubMed]
26. Nixon, S.A.; Welz, C.; Woods, D.J.; Costa-Junior, L.; Zamanian, M.; Martin, R.J. Where are all the anthelmintics? Challenges and opportunities on the path to new anthelmintics. *Int. J. Parasitol.-Drugs Drug Resist.* **2020**, *14*, 8–16. [CrossRef] [PubMed]
27. Charuaud, L.; Jarde, E.; Jaffrezic, A.; Thomas, M.F.; Le Bot, B. Veterinary pharmaceutical residues from natural water to tap water: Sales, occurrence and fate. *J. Hazard. Mater.* **2019**, *361*, 169–186. [CrossRef] [PubMed]
28. Chai, J.-Y.; Jung, B.-K.; Hong, S.-J. Albendazole and Mebendazole as Anti-Parasitic and Anti-Cancer Agents: An Update. *Korean J. Parasitol.* **2021**, *59*, 189–225. [CrossRef] [PubMed]
29. Hegazy, S.K.; El-Azab, G.A.; Zakaria, F.; Mostafa, M.F.; El-Ghoneimy, R.A. Mebendazole; from an anti-parasitic drug to a promising candidate for drug repurposing in colorectal cancer. *Life Sci.* **2022**, *299*, 120536. [CrossRef] [PubMed]
30. Alavi, S.E.; Shahmabadi, H.E. Anthelmintics for drug repurposing: Opportunities and challenges. *Saudi Pharm. J.* **2021**, *29*, 434–445. [CrossRef] [PubMed]
31. Wang, X.; Lou, K.; Song, X.; Ma, H.; Zhou, X.; Xu, H.; Wang, W. Mebendazole is a potent inhibitor to chemoresistant T cell acute lymphoblastic leukemia cells. *Toxicol. Appl. Pharmacol.* **2020**, *396*, 115001. [CrossRef] [PubMed]
32. Elayapillai, S.; Ramraj, S.; Benbrook, D.M.; Bieniasz, M.; Wang, L.; Pathuri, G.; Isingizwe, Z.R.; Kennedy, A.L.; Zhao, Y.D.; Lightfoot, S.; et al. Potential and mechanism of mebendazole for treatment and maintenance of ovarian cancer. *Gynecol. Oncol.* **2021**, *160*, 302–311. [CrossRef] [PubMed]
33. Duan, Q.; Liu, Y.; Rockwell, S. Fenbendazole as a Potential Anticancer Drug. *Anticancer Res.* **2013**, *33*, 355–362. [PubMed]
34. Abubakar, Y.; Tijjani, H.; Egbuna, C.; Adetunji, C.O.; Kala, S.; Kryeziu, T.L.; Ifemeje, J.C.; Patrick-Iwuanyanwu, K.C. Pesticides, History, and Classification. In *Natural Remedies for Pest, Disease and Weed Control*; Egbuna, U.C., Sawicka, B., Eds.; Academic Press: Amsterdam, The Netherlands, 2019; pp. 29–42. [CrossRef]
35. El-Nahhal, I.; El-Nahhal, Y. Pesticide residues in drinking water, their potential risk to human health and removal options. *J. Environ. Manag.* **2021**, *299*, 113611. [CrossRef] [PubMed]
36. Smith, E.H.; Kennedy, G.G. History of Pesticides. In *Encyclopedia of Pest Management*; Pimentel, D., Ed.; Informa Taylor & Francis Group: London, UK, 2002.
37. Kalyabina, V.P.; Esimbekova, E.N.; Kopylova, K.V.; Kratasyuk, V.A. Pesticides: Formulants, Distribution Pathways and Effects on Human Health—A Review. *Toxicol. Rep.* **2021**, *8*, 1179–1192. [CrossRef] [PubMed]
38. Chave, P.A. Pesticides in Freshwaters from Arable Use. In *Pesticides—Developments, Impacts and Controls*; Best, G., Ruthven, D., Eds.; Royal Society of Chemistry: Cambridge, UK, 1995; pp. 100–111.
39. Chavoshani, A.; Hashemi, M.; Amin, M.M.; Ameta, S.C. Risks and challenges of pesticides in aquatic environments. In *Micropollutants and Challenges: Emerging in the Aquatic Environments and Treatment Processes*; Munro, U.L., Ed.; Elsevier: Amsterdam, The Netherlands, 2020; pp. 179–213. [CrossRef]
40. Capoferri, D.; Della Pelle, F.; Del Carlo, M.; Compagnone, D. Affinity sensing strategies for the detection of pesticides in food. *Foods* **2018**, *7*, 148. [CrossRef] [PubMed]

41. Cimino, A.M.; Boyles, A.L.; Thayer, K.A.; Perry, M.J. Effects of neonicotinoid pesticide exposure on human health: A systematic review. *Environ. Health Perspect.* **2017**, *125*, 155–162. [CrossRef] [PubMed]
42. Zhong, G.; Xie, Z.; Cai, M.; Möller, A.; Sturm, R.; Tang, J.; Zhang, G.; He, J.; Ebinghaus, R. Distribution and air-sea exchange of current-use pesticides (CUPs) from East Asia to the high Arctic Ocean. *Environ. Sci. Technol.* **2012**, *46*, 259–267. [CrossRef] [PubMed]
43. Balmer, J.E.; Morris, A.D.; Hung, H.; Jantunen, L.; Vorkamp, K.; Rigét, F.; Evans, M.; Houde, M.; Muir, D.C.G. Levels and trends of current-use pesticides (CUPs) in the arctic: An updated review, 2010–2018. *Emerg. Contam.* **2019**, *5*, 70–88. [CrossRef]
44. Pistorius, J.; Bischoff, G.; Heimbach, U.; Stähler, M. Bee poisoning incidents in Germany in Spring 2008 caused by abrasion of active substance from treated seeds during sowing of maize. *Julius-Kuhn-Archiv* **2009**, *423*, 118–126.
45. Boyd, W.A.; Boyles, A.L.; Blain, R.B.; Skuce, C.R.; Engstrom, A.K.; Walker, V.R.; Thayer, K.A.; Rooney, A.A. *NTP Research Report on the Scoping Review of Potential Human Health Effects Associated with Exposures to Neonicotinoid Pesticides*; Research Report; National Toxicology Program: Research Triangle Park, NC, USA, 2020.
46. Bandeira, F.O.; Alves, P.R.L.; Hennig, T.B.; Brancalione, J.; Nogueira, D.J.; Matias, W.G. Chronic effects of clothianidin to non-target soil invertebrates: Ecological risk assessment using the species sensitivity distribution (SSD) approach. *J. Hazard. Mater.* **2021**, *419*, 126491. [CrossRef] [PubMed]
47. Zhang, A.-A.; Sutar, P.P.; Bing, Q.; Fang, X.-M.; Ni, J.-B.; Xiao, H.-W. Pesticide residue elimination for fruits and vegetables: The mechanisms, applications, and future trends of thermal and non-thermal technologies. *J. Future Foods* **2022**, *2*, 223–240. [CrossRef]
48. Embrandiri, A.; Kiyasudeen, S.K.; Rupani, P.F.; Ibrahim, M.H. Environmental xenobiotics and its effects on natural ecosystem. In *Plant Responses to Xenobiotics*, 1st ed.; Singh, A., Prasad, S.M., Sing, R.P., Eds.; Springer: Singapore, 2016; pp. str. 1–15. [CrossRef]
49. Ljubas, D.; Čizmić, M.; Vrbat, K.; Stipaničev, D.; Repec, S.; Ćurković, L.; Babić, S. Albendazole Degradation Possibilities by UV-Based Advanced Oxidation Processes. *Int. J. Photoenergy* **2018**, *2018*, 1–6. [CrossRef]
50. Judd, S. *The MBR Book: Principles and Applications of Membrane Bioreactors in Water and Wastewater Treatment*; Elsevier: Oxford, UK, 2006; Volume 1, pp. 22–29.
51. Beier, S.P. *Pressure Driven Membrane Processes*; Bookboon: Copenhagen, Denmark, 2007; Volume 2, pp. 4–5.
52. Košutić, K.; Furač, L.; Sipos, L.; Kunst, B. Removal of arsenic and pesticides from drinking water by nanofiltration mem branes. *Sep. Purif. Technol.* **2005**, *42*, 137–144. [CrossRef]
53. Racar, M.; Dolar, D.; Karadakić, K.; Čavarović, N.; Glumac, N.; Ašperger, D.; Košutić, K. Challenges of municipal wastewater reclamation for irrigation by MBR and NF/RO: Physico-chemical and microbiological parameters, and emerging contaminants. *Sci. Total Environ.* **2020**, *722*, 137959. [CrossRef] [PubMed]
54. Dolar, D.; Košutić, K. Removal of pharmaceuticals by ultrafiltration (UF), nanofiltration (NF), and reverse osmosis (RO) membranes. *Sep. Purif. Technol.* **2011**, *86*, 237–246.
55. Mukherjee, A.; Mehta, R.; Saha, S.; Bhattacharya, A.; Biswas, P.K.; Kole, R.K. Removal of multiple pesticide residues from water by low-pressure thin-film composite membrane. *Appl. Water Sci.* **2020**, *10*, 244. [CrossRef]
56. Tepuš, B.; Simonič, M.; Petrinić, I. Comparison between nitrate and pesticide removal from ground water using adsorbents and NF and RO membranes. *J. Hazard. Mater.* **2009**, *170*, 1210–1217. [CrossRef] [PubMed]
57. Plattner, J.; Kazner, C.; Naidu, G.; Wintgens, T.; Vigneswaran, S. Removal of selected pesticides from groundwater by membrane distillation. *Environ. Sci. Pollut. Res.* **2018**, *25*, 2033620347. [CrossRef] [PubMed]
58. Ates, N.; Uzal, N.; Yetis, U.; Dilek, F.B. Removal of pesticides from secondary treated urban wastewater by reverse osmosis. *Environ. Sci. Pollut. Res.* **2023**, *30*, 8732–8745. [CrossRef] [PubMed]
59. Chen, S.-S.; Taylor, J.S.; Mulford, L.A.; Norris, C.D. Influences of molecular weight, molecular size, flux, and recovery for aromatic pesticide removal by nanofiltration membranes. *Desalination* **2004**, *160*, 103–111. [CrossRef]
60. Dolar, D.; Drašinac, N.; Košutić, K.; Škorić, I.; Ašperger, D. Adsorption of hydrophilic and hydrophobic pharmaceuticals on RO/NF membranes: Identification of interactions using FTIR. *J. Appl. Polym. Sci.* **2017**, *134*, 44426. [CrossRef]
61. Li, Y.; Su, P.; Li, Y.; Wen, K.; Bi, G.; Cox, M. Adsorption-Desorption and Degradation of Insecticides Clothianidin and Thiamethoxam in Agricultural Soils. *Chemosphere* **2018**, *207*, 708–714. [CrossRef] [PubMed]
62. Cano, P.A.; Jaramillo-Baquero, M.; Zúñiga-Benítez, H.; Londoño, Y.A.; Peñuela, G.A. Use of Simulated Sunlight Radiation and Hydrogen Peroxide in Azithromycin Removal from Aqueous Solutions: Optimization & Mineralization, Analysis. *Emerg. Contam.* **2020**, *6*, 53–61. [CrossRef]
63. Dolar, D.; Vuković, A.; Ašperger, D.; Košutić, K. Effect of water matrices on removal of veterinary pharmaceuticals by nanofiltration and reverse osmosis membranes. *J. Environ. Sci.* **2011**, *23*, 1299–1307. [CrossRef] [PubMed]
64. Babić, B.; Andrić, D.; Farkaš, A.; Vuk, D.; Ašperger, D.; Dolar, D. Behavior of Mebendazole during NF/RO Adsorption and Photolysis. *Membranes* **2022**, *12*, 888. [CrossRef] [PubMed]
65. Plakas, K.V.; Karabelas, A.J. Membrane retention of herbicides from single and multi-solute media: The effect of ionic environment. *J. Membr. Sci.* **2008**, *320*, 325–334. [CrossRef]

66. *The Merck Index: An Encyclopedia of Chemicals, Drugs, and Biologicals*, 13th ed.; O'Neil, M.J., Ed.; Merck Research Laboratories: Whitehouse Station, NJ, USA, 2001.
67. Putri, Z.S.; Sato, T.; Yohannes, Y.B.; Ikenaka, Y.; Yamamuro, M. Neonicotinoid detection in rainwater in Japan. *Environ. Monit. Contam. Res.* **2025**, *5*, 57–65. [CrossRef]
68. *DIN 38412-34:1997-07*; German Standard Methods for the Examination of Water, Waste Water and Sludge—Bio-Assays (Group L)—Part 34: Determination of the Inhibitory Effect of Waste Water on the Light Emission of Photobacterium phosphoreum; Luminescent Bacteria Waste Water Test Using Conserved Bacteria (L 34). Deutsches Institut für Normung: Berlin, Germany, 1997.
69. *DIN 38412-341:1993-10*; German Standard Methods for the Examination of Water, Waste Water and Sludge—Bio-Assays (Group L)—Determination of the Inhibitory Effect of Waste Water on the Light Emission of Photobacterium phosphoreum; Luminescent Bacteria Waste Water Test; Extension to the Method DIN 38412-L34 (L 341). Deutsches Institut für Normung: Berlin, Germany, 1993.
70. *ISO 11348-1:2007*; Water Quality—Determination of the Inhibitory Effect of Water Samples on the Light Emission of Vibrio fischeri (Luminescent Bacteria Test)—Part 1: Method Using Freshly Prepared Bacteria. International Organization for Standardization: Geneva, Switzerland, 2007.
71. Breite, D.; Went, M.; Prager, A.; Schulze, A. The critical zeta potential of polymer membranes: How electrolytes impact membrane fouling. *RSC Adv.* **2016**, *6*, 98180–98190. [CrossRef]
72. Zhang, Y.; Zhang, Z.; Yang, J.; Yue, Y.; Zhang, H. A Review of Recent Advances in Superhydrophobic Surfaces and Their Applications in Drag Reduction and Heat Transfer. *Nanomaterials* **2021**, *12*, 44. [CrossRef] [PubMed]
73. Nghiem, L.D.; Schaefer, A.I.; Elimelech, M. Role of electrostatic interactions in the retention of pharmaceutically active contaminants by a loose nanofiltration membrane. *J. Membr. Sci.* **2006**, *286*, 52–59. [CrossRef]
74. Nghiem, L.D.; Schäfer, A.I.; Elimelech, M. Pharmaceutical retention mechanisms by nanofiltration membranes. *Environ. Sci. Technol.* **2005**, *39*, 7698–7705. [CrossRef] [PubMed]
75. Leo, A.; Hansch, C.; Elkins, D. Partition coefficients and their uses. *Chem. Rev.* **1971**, *71*, 525–616. [CrossRef]
76. Nandiyanto, A.B.D.; Oktiani, R.; Ragadhita, R. How to read and interpret ftir spectroscope of organic material. *Indones. J. Sci. Technol.* **2019**, *4*, 97–118. [CrossRef]
77. Jarusutthirak, C.; Amy, G.; Croué, J.P. Fouling characteristics of wastewater effluent organic matter (EfOM) isolates on NF and UFmembranes. *Desalination* **2002**, *145*, 247–255. [CrossRef]
78. Di Nica, V.; Villa, S.; Finizio, A. Toxicity of individual pharmaceuticals and their mixtures to Aliivibrio fischeri: Experimental results for single compounds and considerations of their mechanisms of action and potential acute effects on aquatic organisms. *Environ. Toxicol. Chem.* **2016**, *36*, 807–814. [CrossRef] [PubMed]
79. Sigurnjak Bureš, M.; Cvetnić, M.; Miloloža, M.; Kučić Grgić, D.; Markić, M.; Kušić, H.; Bolanča, T.; Rogošić, M.; Ukić, Š. Modeling the toxicity of pollutants mixtures for risk assessment: A review. *Environ. Chem. Lett.* **2021**, *19*, 1629–1655. [CrossRef]

Disclaimer/Publisher's Note: The statements, opinions and data contained in all publications are solely those of the individual author(s) and contributor(s) and not of MDPI and/or the editor(s). MDPI and/or the editor(s) disclaim responsibility for any injury to people or property resulting from any ideas, methods, instructions or products referred to in the content.